

# Evaluation of Neutron- and Proton-induced Cross Sections of $^{27}\text{Al}$ up to 2 GeV

Young-Ouk LEE and Jonghwa CHANG  
Korea Atomic Energy Research Institute  
Tokio FUKAHORI and Satoshi CHIBA  
Japan Atomic Energy Research Institute

We have evaluated neutron and proton nuclear data of  $^{27}\text{Al}$  for energies up to 2 GeV. The best set of optical model parameters were obtained above 20 MeV for neutron and above reaction threshold for proton up to 250 MeV with the phenomenological potential forms proposed by Chiba. The transmission coefficients for neutron and proton derived from the optical models are fed into the GNASH code system to calculate angle-energy correlated emission spectra for light ejectiles and gamma rays. For energies above 250 MeV and below 2 GeV, the total, reaction and elastic scattering cross sections were evaluated by an empirical fit and recent systematics. Emitted nucleon and pion were estimated by use of QMD+SDM (Quantum Molecular Dynamics + Statistical Decay Model).

## 1. Introduction

Nuclear data for conventional fission reactors and fusion devices mainly consist of neutron-induced cross sections in energy below 20 MeV. However, recent new applications such as radiation transport simulations of cancer radiotherapy and the accelerator-driven transmutation of nuclear wastes require evaluated nuclear data on neutron- and proton-induced reaction above 20 MeV up to a few GeV.

Currently some evaluation works are underway to make high energy libraries for neutron and proton data above 20 MeV. Among the higher-priority materials being evaluated for such applications, aluminum is important in structure for the accelerator-driven system, and its cross sections are often used as a reference to determine other cross sections.

The optical model provides the basis for theoretical evaluations of nuclear cross sections. It is a convenient means for calculations of reaction, shape elastic and (neutron) total cross sections, and also supplies particle transmission coefficients for Hauser-Feshbach statistical theory analyses. In order to perform nuclear data evaluation without unphysical discontinuities, optical models should cover the whole energy range of interest continuously. For energies above 150 MeV where pion production reaction channel opens, the microscopic nuclear reaction calculations are often performed by using intra-nuclear cascade (INC) model together with macroscopic transport calculations by computer codes such as LCS, LAHET and HERMES. Therefore, separate evaluated nuclear data in ENDF-6 format above pion threshold energy are not as abundant as those for energies below 150 MeV when consistency and integrity of evaluated data are to be checked.

Under these circumstances, we evaluated neutron-induced nuclear data of  $^{27}\text{Al}$  for energies above 20 MeV up to 2 GeV, and proton-induced nuclear data above threshold up to 2 GeV.

## 2. Evaluations up to 250 MeV

### (1) Optical Model Analyses

Evaluation starts with determination of global optical model parameters of neutron and proton for aluminum to describe measured total, reaction and elastic scattering cross sections. As a reference data set, we collected measured total (or reaction for proton) cross sections and elastic angular distributions from the EXFOR at NEA Data Bank. The potential form factor was chosen to be of Woods-Saxon form for  $V_r$  and  $W_v$ , derivative Wood-Saxon for  $W_d$  and Thomas-Fermi form for spin-orbit parts as

$$U(r) = -V_r f_v(r) - iW_v f_w(r) + 4i a_{wd} W_d \frac{df_{wd}(r)}{dr} \quad (1)$$

$$- \frac{1}{r} \left( \frac{\hbar}{m_\pi c} \right)^2 \left( V_{so} \frac{d}{dr} f_{iso}(r) + iW_{so} \frac{d}{dr} f_{us0}(r) \right) \mathbf{l} \cdot \mathbf{s} ,$$

where  $m_\pi$  is the mass of pion and the form factors  $f$  are of the standard Woods-Saxon shape :

$$f_i(r) \equiv \frac{1}{1 + \exp((r - r_i A^{1/3})/a_i)} . \quad (2)$$

Here, the  $a_x$  is the diffuseness parameter, and  $A$  the target mass number.

We adopted following potential energy dependencies which are similar to that proposed by Delaroche et al.[1]:

$$V_r(E) = V_0 e^{-\lambda_v(E-E_f)} + V_1 + V_2 E \quad r_v(E) = r_{v0} + r_{v1} E \quad a_v(E) = a_{v0} + a_{v1} E$$

$$W_v(E) = W_{v0} \frac{(E-E_f)^4}{(E-E_f)^4 + W_{v1}^4} \quad r_{wv}(E) = r_v(E) \quad a_{wv}(E) = a_v(E)$$

$$W_d(E) = W_{d0} e^{\lambda_w(E-E_f)} \frac{(E-E_f)^4}{(E-E_f)^4 + W_{d1}^4} \quad r_{wd}(E) = r_{wd0} + r_{wd1} E \quad a_{wd}(E) = a_{wd0} + a_{wd1} E \quad (3)$$

where the Fermi energy  $E_f$  for neutron is given by

$$E_f(Z, A) = -\frac{1}{2} [S_n(Z, A) + S_n(Z, A+1)] \quad (4)$$

with  $S_n$  the neutron separation energy, and for protons by

$$E_f(Z, A) = -\frac{1}{2} [S_p(Z, A) + S_p(Z+1, A+1)] \quad (5)$$

with  $S_p$  the proton separation energy.

The potential parameters of spin-orbit form parts were taken from Delaroche et al.[1] as

$$V_{so}(E) = 6.0 e^{-0.005E} \quad W_{so}(E) = 0.2 - 0.011E$$

$$r_{iso}, w_{iso} = 1.017 \quad a_{iso}, a_{us0} = 0.60 \quad (6)$$

The energy dependent parameters are determined through adjusting the coefficients defined in eq. (3) by use of ECISLOT[2], an interactive optical parameter searcher with simulated annealing algorithm, developed by one of authors.

## (2) Emission Cross Sections

Compound reaction calculations with preequilibrium corrections were performed by using the GNASH[3] code based on the exciton model of Kalbach, discrete level data from nuclear data sheets, continuum level densities using the formulation of Ignatyuk and pairing and shell parameters from the Cook analysis. Besides neutron and proton potentials, the following global potentials were employed in the evaluations for composite particles:

- Deuterons : Perey and Perey[4]
- Tritons : Becchetti and Greenlees[5]
- Alphas : Arthur and Young[6]

The transmission coefficients for neutron and protons calculated from the optical model analyses as well as for deuteron, triton and alpha particles are fed into the GNASH to evaluate angle-energy correlated emission spectra for light ejectiles and gamma rays. Gamma-ray transmission coefficients were calculated using the Kopecky-Uhl model. Direct reaction contributions to inelastic scattering from discrete states were provided by a DWBA calculation. So the original reaction cross section were reduced by the amount of direct reaction cross sections in GNASH calculation.

## 3. Evaluations up to 2 GeV

### (1) Total and Reaction Cross Sections

Since there are not enough measurements and reliable physics descriptions for optical model

approach above few hundred energies where pion production becomes important, we made an empirical fit with available measurements and applied a systematics for total and reaction cross sections.

For neutron and proton reaction cross sections, we adopted the recent systematics developed by NASA[7]. The NASA systematics has following form for the reaction cross section:

$$\sigma_R = \pi r_0^2 (A_P^{1/3} + A_T^{1/3} + \delta_E)^2 \left(1 - \frac{B}{E_{cm}}\right), \quad (7)$$

where  $r_0 = 1.1$  fm,  $A_P$  and  $A_T$  the projectile and target mass numbers and  $E_{cm}$  the colliding system center of mass energy in MeV. Details of parameters  $\delta_E$  (Pauli blocking factor) and  $B$  (energy-dependent Coulomb interaction barrier) are explained in the reference[7]. We applied this systematics first for reaction cross sections for energies from 250 MeV to 2 GeV, and the results are merged with those obtained from optical model approach below 250 MeV.

For neutron total cross sections, we made a data fitting combined with the NASA systematics for the reaction cross section to describe measured data as:

$$\sigma_T(E) = \sigma_R(E) \cdot (a + b \cdot E), \quad 250 \text{ MeV} < E < 2000 \text{ MeV}. \quad (8)$$

and again the results were merged with those obtained from optical model approach below 250 MeV.

## (2) Emission of nucleons above Pion Threshold

To evaluate emission of nucleons for energies above pion production threshold, we tried QMD+SDM[8,9] instead of well-known INC (Intra Nuclear Cascade) model to calculate nucleon emission spectra for incident neutron and proton of energies above 150 MeV up to 2 GeV.

This model is based on quantum molecular dynamics (QMD) incorporated with a statistical decay model (SDM) to describe various nuclear reaction in a unified way. INC and pre-equilibrium processes are described by QMD model, and equilibrium process by SDM. The details of the QMD+SDM calculations are given in Ref. [8,9].

## 4. Results and Comparisons

### (1) Optical Model and Total, Reaction and Elastic Cross Sections up to 250 MeV

Figure 1 show the resulting potential depths of real and imaginary volume as a function of both neutron and proton energies obtained by use of ECISPLOT. The proton depths for real and imaginary potentials are shown to be higher than that of neutron. Table 1 lists finally optimized coefficients giving two sets of potential depths and form functions for neutron and proton that describe the reference experimental data with minimum variance. The total (for neutron), reaction (for proton) cross sections and elastic angular distributions resulted from optical model analyses are shown in Figs. 2-5, with various measurements, and compared with JENDL and LANL evaluations up to 250 MeV. Our optical model parameters give excellent agreements with most of experimental data over entire energy range for both incident neutron and proton.

### (2) Emission Cross Sections up to 250 MeV

Figure 6 compares the evaluated Na-23 isotope production cross sections of incident neutron against Los Alamos data together with evaluations from LANL and JENDL. The production cross sections consists of emission reactions of (n,na), (n,dt), (n,npt), (n,n2d), (n,2npd) and (n,3n2p) to give the residual Na-23 isotope. Our evaluated cross sections sections and other two evaluated ones give good agreements with the measured data in energies from the threshold up to 45 MeV. Around the neutron energy of 22 MeV having peak cross sections, our evaluations are slightly closer to the measurements than the other two. Above the neutron energy of 45 MeV, all evaluated cross sections have similar values to have lower cross sections than the measurements.

### (3) Total and Reaction Cross Sections up to 2 GeV

The dotted line in Fig. 7 shows the evaluated reaction cross sections of neutron up to 2 GeV consisting of the optical model calculations and NASA systematics (eq. (7)), together with various measurements. The good agreement is shown between the evaluation and the data except mismatches in the energies around 400 MeV where the measured data are considered to have larger errors than reported. Our evaluations around these energies could be validated by the consistency with the evaluated neutron total cross sections which are described next.

The solid line in Fig. 7 shows the evaluated total cross section of neutron up to 2 GeV consisting of the optical model calculations and data fitting using eq. (8), together with available measurements. The evaluated neutron total cross sections reproduced most of measured data well except one point at 1731 MeV, which has largest errors among all data points. Our evaluation for neutron total cross sections validates the evaluated neutron reaction cross sections which show consistent behaviour with both measured and evaluated total cross sections despite of the mismatches for some measured data around 400 MeV mentioned earlier.

Solid line in Fig. 8 shows the evaluated reaction cross sections of proton up to 2 GeV merged from the optical model calculations and NASA systematics (eq. (7)), together with various measurements and LANL evaluations with dotted line. The evaluated reaction cross sections agree well with all of measured data.

#### (4) Emission of nucleons above Pion Threshold

Figure 9 shows our evaluation by use of QMD+SDM for neutron emission spectra for the reaction of 597 MeV proton with  $^{27}\text{Al}$  at different laboratory angles, compared with the measurements from Juelich. As shown in the figure, the evaluated neutron spectra at all directions reproduce well the measured data except the higher energy emissions in 30 degree angle. In Fig. 10, QMD+SDM evaluations are presented for the negative pion emission spectra for the reaction of 585 MeV proton with  $^{27}\text{Al}$  at 5 different laboratory angles together with the measured data from Juelich. The evaluated pion spectra give an overall agreement with the measured data for all directions.

The results presented above give us an applicability of QMD+SDM for producing separate evaluated data, especially for nucleon emission spectra in energies above pion production threshold as an alternative to the INC model codes combined with macroscopic transport calculations.

## 5. Conclusion

We evaluated the neutron and proton cross sections of  $^{27}\text{Al}$  which is important in shielding and structural material for accelerator-driven system for energies up to 2 GeV. Optimized potential parameters describes well the experimental data of total, reaction cross section and elastic angular distributions. The resulting transmission coefficients of neutron and proton are fed into the GNASH code to evaluate production cross sections of residual nuclei and angle-energy correlated emission spectra for light ejectiles with  $A \leq 4$  and gamma rays. Some of cross sections from GNASH calculations were compared with experimental data, giving good agreements. For energies above 250 MeV up to 2 GeV, the total and reaction cross sections were evaluated by an empirical fit and recent systematics. The neutron, proton and pion emission spectra for energies above pion production threshold energy were estimated by use of QMD+SDM.

## References

- [1] Delaroche, J.P., Wang, Y., J. Rapaport: Phys. Rev. **C39**, 391 (1989)
- [2] Lee, Y.O., et al.: "ECISLOT: Interactive Optical Model Searcher with Simulated Annealing Algorithm", to be published.
- [3] Young, P.G., Arthur, E.D., Chadwick, M. B.: "Comprehensive Nuclear Model Calculations: Introduction to the Theory and Use of the GNASH Code," LA-12343-MS (1992).

- [4] Perey, C.M., Perey, F.G.: Phys. Rev. **132**, 755 (1963)  
 [5] Becchetti, F.D. Jr., Greenlees, G.W.: "Polarization Phenomena in Nuclear Reactions", (Ed: H.H. Barschall and W. Haeberli, The University of Wisconsin Press,1971) p.682.  
 [6] Young, P.G.: IAEA INDC(NDS)-335 p.109 (1995)  
 [7] Tripathi, R.K., et al.: "Universal Parameterization of Absorption Cross Sections" , NASA Technical Paper 3621, Jan. 1997.  
 [8] Niita, K., et al.: Phys. Rev., **C52**, 2620 (1995)  
 [9] Chiba, S., et al.: Phys. Rev., **C54**, 285 (1996)

Table 1. Optical potential parameters for n,p +  $^{27}\text{Al}$  interaction up to 250 MeV.

	$V_0$ (MeV)	$\lambda_{vr}$ ( $\text{MeV}^{-1}$ )	$V_1$ (MeV)	$V_2$ ( $\text{MeV}^{-1}$ )	$r_{v0}$ (fm)	$r_{v1}$ (fm/MeV)	$a_{v0}$ (fm)	$a_{v1}$ (fm/MeV)
<b>Neutron</b>	109.8	0.006	-48.27	0.168	1.190	0.00013	0.627	0.0004
<b>Proton</b>	111.0	0.007	-44.87	0.176	1.153	0.00016	0.552	0.0016

	$W_{u0}$ (MeV)	$W_{u1}$ (MeV)	$\lambda_{ud}$ ( $\text{MeV}^{-1}$ )	$W_{d0}$ (MeV)	$W_{d1}$ (MeV)	$r_{wd0}$ (fm)	$r_{wd1}$ (fm/MeV)	$a_{wd0}$ (fm)	$a_{wd1}$ (fm/MeV)
<b>neutron</b>	10.58	41.50	0.065	46.50	18.32	1.06	0.0	0.62	0.0008
<b>proton</b>	10.89	35.86	0.057	38.91	28.09	1.30	0.0	0.60	0.0

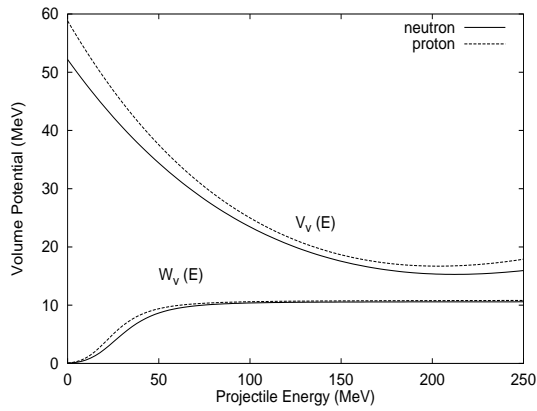


Fig. 1. The real volume potential depths as a function of neutron and proton energy for aluminum

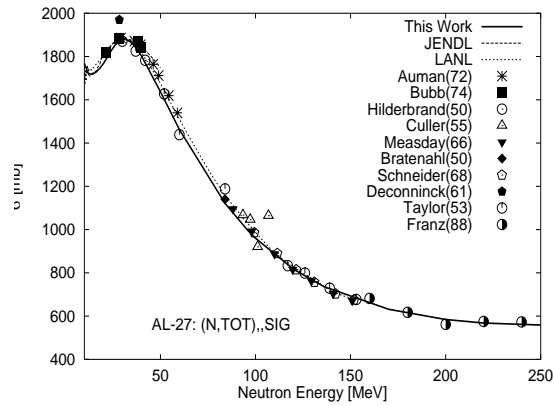


Fig. 2. Total cross sections of neutron for  $^{27}\text{Al}$  from optimized optical potential parameters for energies up to 250 MeV

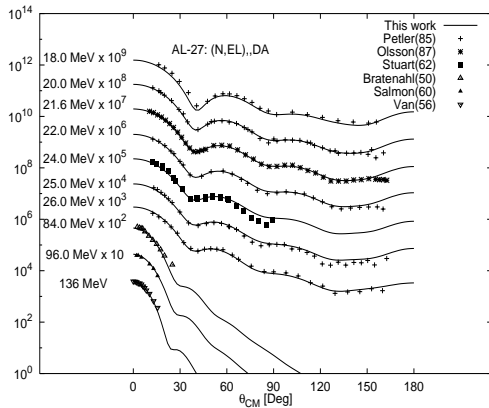


Fig. 3 Elastic angular distributions of neutron for  $^{27}\text{Al}$  from optimized optical potential parameters for energies up to 250 MeV

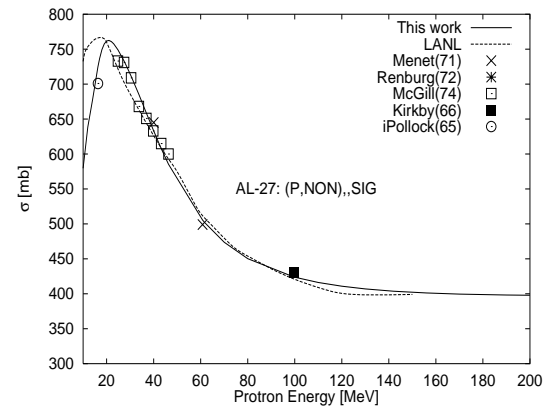


Fig. 4 Reaction cross sections of proton for  $^{27}\text{Al}$  from optimized optical potential parameters for energies up to 250 MeV

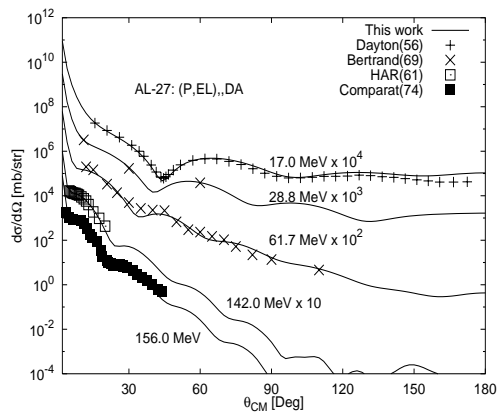


Fig. 5 Elastic angular distributions of proton for  $^{27}\text{Al}$  from optimized optical potential parameters compared with measurements for energies up to 250 MeV

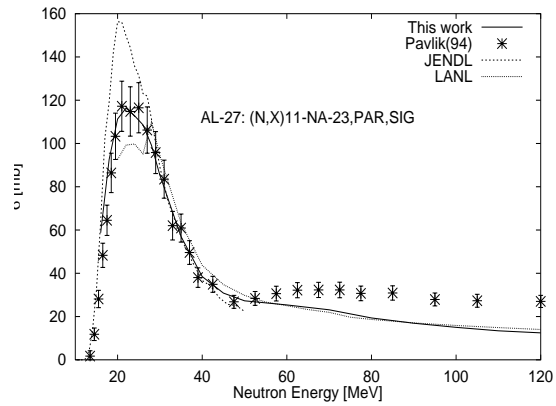


Fig. 6 Evaluated Na-23 production cross sections of neutron for  $^{27}\text{Al}$ . Reactions included: (n,na), (n,dt), (n,npt), (n,n2d), (n,2npd), (n,3n2p), (n,n2d) (n,2npd) (n,3n2p)

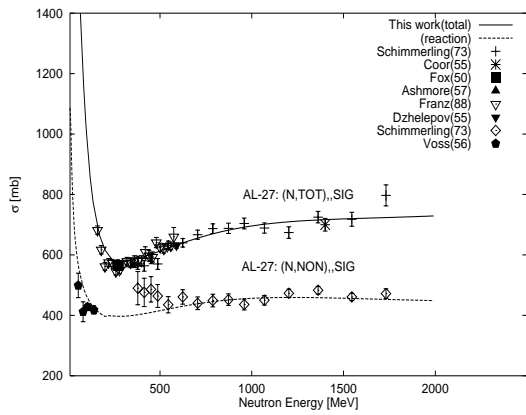


Fig. 7 Neutron total and reaction cross sections up to 2 GeV for  $^{27}\text{Al}$

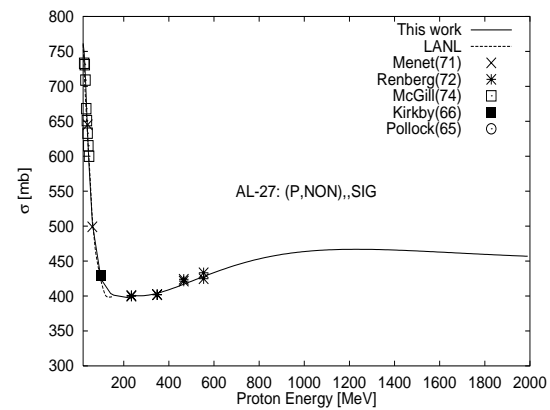


Fig. 8 Proton reaction cross sections up to 2 GeV for  $^{27}\text{Al}$

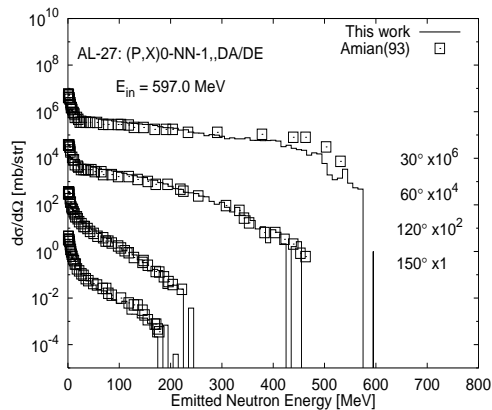


Fig. 9 Neutron emission spectra from the reaction of proton (597 MeV) +  $^{27}\text{Al}$  at different laboratory angles

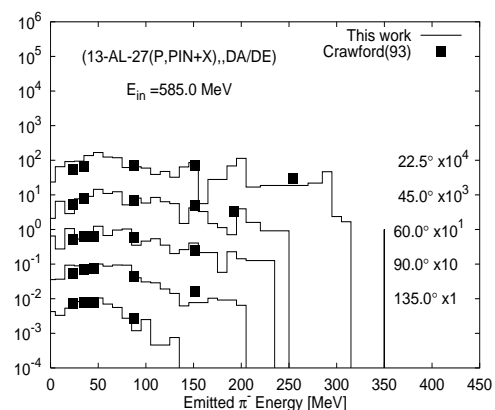


Fig. 10 Negative pion emission spectra from the reaction of proton (585 MeV) +  $^{27}\text{Al}$  at different laboratory angles